Tetrahedron: *Asymmetry*

Pergamon

TETRAHEDRON: *ASYMMETRY*

Enantioselective Michael Addition of Isobutyraldehyde to Nitroalkenes Organocatalyzed by Chiral Primary Amine-Guanidines

Angel Avila[a], Rafael Chinchilla[a,*], Béla Fiser,[b] Enrique Gómez-Bengoa[b], Carmen Nájera[a,*]

[a] *Departamento de Química Orgánica, Facultad de Ciencias, and Instituto de Síntesis Orgánica (ISO), Universidad de Alicante, Apdo. 99, 03080 Alicante, Spain*

[b] *Departamento de Química Orgánica I, Universidad del País Vasco, Apdo. 1072, 20080 San Sebastián, Spain*

Abstract— Primary amine-guanidines derived from *trans*-cyclohexane-1,2-diamines are used as organocatalysts for the enantioselective conjugate addition of isobutyraldehyde to arylated and heteroarylated nitroalkenes. The reaction is performed in the presence of imidazole as additive in aqueous DMF as solvent at 0 ºC. The corresponding Michael adducts bearing a new stereocenter are obtained in high yields with enantioselectivities up to 80%. Theoretical calculations are used to justify the observed sense of the stereoinduction.

1. Introduction

γ-Nitrocarbonyl compounds have gained a great importance during recent years as key precursors of various important compounds such as alkaloids,[1] aminoacids,[2] antitumorals,[3] antibiotics,[4] peptido-mimetics,[5] and marine metabolites[6] among others.[7] Nowadays, the enantioselective Michael addition reaction of enolizable carbonyl compounds to nitroalkenes promoted by a chiral organocatalyst is one of the most common and convenient procedures for achieving the synthesis of γ-nitrocarbonyl compounds in an enantiomerically enriched form.[8] Thus, organocatalysts with bifunctional characteristics have been the most efficient for the enantioselective addition reaction of aldehydes or ketones to nitroolefins, particularly those containing a primary amine and a thiourea moiety.[9] For instance, the enantioselective Michael addition reaction of aldehydes to nitroalkenes has been successfully performed using as organocatalysts the chiral *trans*-cyclohexane-1,2-diamine-derived primary amine-thioureas **1**,[10] **2**[11] and **3**,[12] as well as the *Cinchona*-derived **4**,[13] the isosteviol-derived **5**[14] and even calix[4]arene-derived compounds.[15] Using all these primary amine-containing organocatalysts, the enantioselectivity is induced by addition of a transient enamine to the nitroolefin, which is hydrogen bond-coordinated by the nitro group to the NH groups of the thiourea.

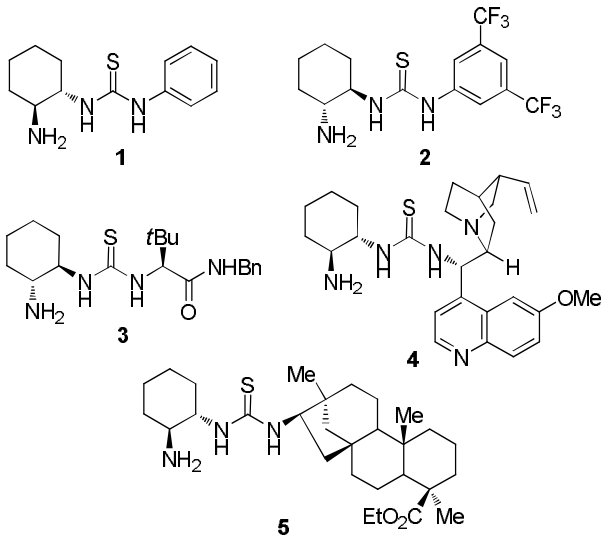

We have recently reported the synthesis of primary amine-guanidines **6** and *ent*-**6a** from chiral *trans*-cyclohexane-1,2-diamines and their use as organocatalysts in the enantioselective Michael addition reaction of aldehydes, mainly α,α-disubstituted, to maleimides.[16] Is this paper we explore the use of these primary amine-guanidines **6** as chiral organocatalysts in the conjugate addition reaction of a α,α-disubstituted aldehydes such as isobutyraldehyde to nitroalkenes, leading to enantioenriched γ-nitroaldehydes. In addition, theoretical calculations have been used to explain the observed enantioselectivity.

* Corresponding author. Tel.: +34-96-5903728; fax: +34-96-5903549; e-mail: chinchilla@ua.es (R. Chinchilla), cnajera@ua.es (C. Nájera).

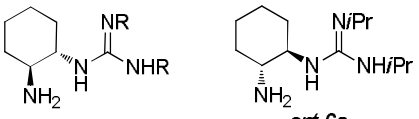

6a, R = *i*Pr
6b, R = Cy

ent-**6a**

2. Results and discussion

The primary amine-guanidines **6a** and **6b** employed as organocatalysts in this study were prepared as previously reported[16b] by monoguanylation of (1*S*,2*S*)-cyclohexane-1,2-diamine with *N*,*N*'-diisopropylcarbodiimide or *N*.*N*'-dicyclohexylcarbodiimide, respectively. The search for the most appropriate reaction conditions (Table 1) began with the Michael addition reaction of isobutyraldehyde (**7**) to *trans*-β-nitrostyrene (**8a**), organocatalyzed by **6a** (20 mol%) in toluene as solvent at room temperature, which afforded the corresponding adduct (*R*)-**9a** in only 22% yield and with a modest 53% *ee* after 5 d reaction time (Table 1, entry 1). The (*R*) absolute configuration of the final adduct was determined by comparison of the elution order of the corresponding enantiomers in chiral HPLC with those in the literature.[17]

The addition of imidazole as basic additive, something that proved beneficial when **6a** organocatalyzed the Michael addition reaction of aldehydes to maleimides,[16b] was again effective, increasing the reactivity of the process and allowing the isolation of (*R*)-**9a** in 92% yield in the same reaction time athough in a lower *ee* (Table 1, entry 2). The use of de dicyclohexyl-containing primary amine-guanidine **6b** as organocatalyst under these reaction conditions resulted in a much lower yield and enentioselectivity for (*R*)-**9a** (Table 1, entry 3), therefore the study continued organocatalyzed by **6a**. Thus, the use of other solvents such as acetone, *tert*-butyl methyl ether or methanol gave high yields for (*R*)-**9a** in 5 d reaction time, but only 34, 53 and 35% *ee's*, respectively (Table 1, entries 4-6), whereas the use of nitromethane as solvent gave **9a** as a racemic mixture (Table 1, entry 7).

However, the use of DMF as solvent increased dramatically the reaction rate, affording quantitatively (*R*)-**9a** in 48% *ee* (Table 1, entry 8). The increasing reaction rate was also observed when water was used as solvent, but now the enantioselectivity of the process raised up to 71%, adduct (*R*)-**9a** being isolated in 80% yield (Table 1, entry 9). Therefore, mixtures of DMF/H_2O were assayed as solvents, attempting to combine the beneficial effects of both solvents. Thus, the use of a DMF/H_2O mixture in a 2:1 (v/v) ratio as solvent gave rise to a quantitative yield of (*R*)-**9a** in 62% *ee* (Table 1, entry 10). Increasing the amount of water from 1/2 to 1/4 (v/v) ratios resulted in higher enantioselectivities for (*R*)-**9a** (67 and 70%, respectively) while keeping the quantitative yield (Table 1, entries 11 and 12).

Table 1. Screening and optimization of the reaction conditions for the enantioselective Michael addition.

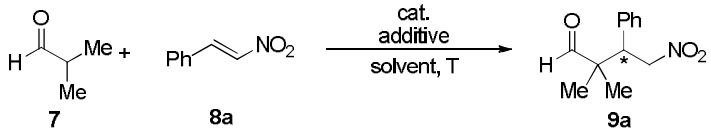

7 **8a** **9a**

Entry	Catalyst (mol%)	Additive (mol%)[a]	Solvent	*T* (ºC)	*t* (d)	Yield (%)[b]	*ee* (%)[c]
1	**6a** (20)	-	PhMe	25	5	22	53 (*R*)
2	**6a** (20)	Imidazole (20)	PhMe	25	5	92	44 (*R*)
3	**6b** (20)	Imidazole (20)	PhMe	25	5	30	27 (*R*)
4	**6a** (20)	Imidazole (20)	Acetone	25	5	96	34 (*R*)
5	**6a** (20)	Imidazole (20)	TBME	25	5	96	53 (*R*)
6	**6a** (20)	Imidazole (20)	MeOH	25	5	99	35 (*R*)
7	**6a** (20)	Imidazole (20)	$MeNO_2$	25	5	74	0
8	**6a** (20)	Imidazole (20)	DMF	25	0.7	99	48 (*R*)
9	**6a** (20)	Imidazole (20)	H_2O	25	0.7	80	71 (*R*)
10	**6a** (20)	Imidazole (20)	DMF/H_2O[d]	25	0.7	99	62 (*R*)
11	**6a** (20)	Imidazole (20)	DMF/H_2O[e]	25	0.7	99	67 (*R*)
12	**6a** (20)	Imidazole (20)	DMF/H_2O[f]	25	0.7	99	70 (*R*)
13	**6a** (20)	TEA (20)	DMF/H_2O[f]	25	0.7	97	60 (*R*)
14	**6a** (20)	DBU (20)	DMF/H_2O[f]	25	0.7	90	33 (*R*)
15	**6a** (20)	DABCO (20)	DMF/H_2O[f]	25	0.7	85	70 (*R*)
16	**6a** (20)	$PhCO_2H$ (20)	DMF/H_2O[f]	25	0.7	5	63 (*R*)
17	**6a** (10)	Imidazole (10)	DMF/H_2O[f]	25	3	99	70 (*R*)
18	**6a** (20)	Imidazole (20)	DMF/H_2O[f]	0	2	90	80 (*R*)
19	*ent*-**6a** (20)	Imidazole (20)	DMF/H_2O[f]	0	2	87	80 (*S*)

[a] TEA: Triethylamine; DBU: 1,8-Diazabicyclo[5.4.0]undec-7-ene; DABCO: 1,4-Diazabicyclo[2.2.2]octane.

[b] Isolated yield after flash chromatography.

[c] Enantioselectivities and absolute stereochemistry determined by chiral HPLC (Ref. 8b).

[d] 2/1, v/v.

[e] 1/2, v/v.

[f] 1/4, v/v.

The use of other basic additives (20 mol%) in the reaction using the most appropriate solvent [DMF/H_2O, 1/4 (v/v)] were also assayed. Thus, the use of triethylamine or 1,8-diazabicyclo[5.4.0]undec-7-ene (DBU) afforded lower enantioselections for (*R*)-**9a** (Table 1, entries 13 and 14), whereas when 1,4-diazabicyclo[2.2.2]octane (DABCO) was used as additive, a similar *ee* than when using imidazole was observed, although the reaction was not quantitative (Table 1, entry 15). In addition, when an acid additive such as benzoic acid was assayed, almost no reaction was observed (Table 1, entry 16). Moreover, when the organocatalyst **6a** and the imidazole additive loadings were lowered down to 10 mol%, adduct (*R*)-**9a** was isolated quantitatively in 70% *ee*, but the reaction time increased considerably (Table 1, entry 17).

Attempting to increase the enantioselectivity of the process, we also lowered down the reaction temperature. Thus, when the process was carried out at 0 ºC, the reaction time increased to 2 d, but the enantioselectivity of adduct (*R*)-**9a** raised up to 80%, being isolated in 90% yield (Table 1, entry 18).

Expecting to achieve an opposite enantioselection, we also performed the reaction using as organocatalyst *ent*-**6a**, which can be prepared similarly to its enantiomeric counterpart, but using (1*R*,2*R*)-cyclohexane-1,2-diamine as chirality source.[16b] Using this primary amine-guanidine as catalyst (20 mol%) under the most effective reaction conditions [imidazole as additive (20 mol%), DMF/H_2O, 1/4 (v/v), 0 ºC], the expected adduct (*S*)-**9a** was isolated in 80% *ee* (Table 1, entry 19).

Next we explore the addition reaction of isobutyraldehyde to other trans-β-nitroalkenes **8** under the most favourable reaction conditions [**6a** (20 mol%), imidazole (20 mol%), DMF/H_2O, 1/4 (v/v), 0 ºC], the results being summarized in Table 2. Thus, when nitroalkenes **8b** and **8c**, bearing electron-releasing groups such as methyl or methoxy in the aromatic ring, were used, the corresponding Michael adducts (*R*)-**9b** and (*R*)-**9c** were isolated in good yields and with enantioselectivities of 80 and 75%, respectively (Table 2, entries 2 and 3). The presence of halogen groups onto the aromatic ring of the nitroalkene such as fluoro (**8d**), chloro (**8e**) and bromo (**8f**) showed a certain influence in the enantioselectivity of the process, the corresponding adducts (*R*)-**9d**, (*R*)-**9e** and (*R*)-**9f** being obtained with diminishing *ee*'s down to 65% as the electronegativity of the group is reduced (Table 2, entries 4-6). This apparent beneficial influence of the presence of electron-withdrawing groups in the aromatic ring of the nitroalkene was confirmed when a nitro group was present (**8g**), the reaction affording adduct (*R*)-**9g** in 80% ee (Table 2, entry 7).

When nitroalkene **9h** bearing a 2-naphthyl group was employed as Michael acceptor, the corresponding adduct (*R*)-**9h** was obtained in 70% *ee* (Table 2, entry 8). In addition, the influence of the presence of heteroarylated rings in the nitroalkene was also explored with the use as Michael acceptors of the 3-pyridinyl- and 2-furanyl-containing nitroalkenes **8i** and **8j**, which gave rise to adducts (*R*)-**9i** and (*R*)-**9j** in 80 and 70% *ee*, respectively (Table 2, entries 8 and 10).

The absolute configuration of the known γ-nitroaldehydes **9** was assigned according to the elution order of their enantiomers in chiral HPLC when compared to the literature (see Experimental).

Table 2. Enantioselective Michael addition of isobutyraldehyde to nitroalkenes organocatalyzed by **6a**.

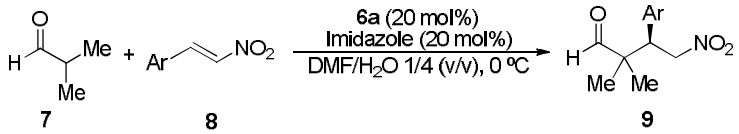

7 8 9

Entry	Nitroalkene		*t* (d)	Adduct No.	Yield (%)[a]	*ee* (%)[b,c]
	Ar	No.				
1	Ph	**8a**	2	(*R*)-**9a**	90	80
2	4-MeC_6H_4	**8b**	2	(*R*)-**9b**	75	80
3	4-$MeOC_6H_4$	**8c**	2	(*R*)-**9c**	89	75
4	4-FC_6H_4	**8d**	2	(*R*)-**9d**	73	80
5	4-ClC_6H_4	**8e**	2	(*R*)-**9e**	90	75
6	4-BrC_6H_4	**8f**	2	(*R*)-**9f**	70	65
7	4-$O_2NC_6H_4$	**8g**	2	(*R*)-**9g**	85	80
8	2-Naphthyl	**8h**	2	(*R*)-**9h**	75	70
9	3-Pyridinyl	**8i**	2	(*R*)-**9i**	91	80
10	2-Furanyl	**8j**	2	(*R*)-**9j**	95	70

[a] Isolated yield after flash chromatography.

[b] Enantioselectivities determined by chiral HPLC.

[c] Absolute configuration assigned by the order of elution of the enantiomers in chiral HPLC (See Experimental).

In order to get further insight into the origin of the observed enantioselectivity, we carried out DFT theoretical calculations. Our goal was to determine the hydrogen bonding activation pattern of the nitro group, including the role of the pendant guanidine moiety and the role of water beyond just being the solvent of the reaction. We assumed that the initial formation of an enamine between the primary amine of the catalyst **6a** and the aldehyde **7** is followed by nucleophilic attack to nitrostyrene **8a** following Seebach´s synclinal model.[18] At that point, the partial negative charge developing in the nitro group during the C-C bond forming transition state might be stabilized by hydrogen bonding with the guanidine (TS_H-S and TS_H-R, Figure 1), or alternatively, stabilized and solvated by the surrounding water molecules (TS_W-S).

As could be anticipated from our previous report on the related Michael addition catalyzed by **6a**,[16b] we found that if only intramolecular H-bonding was taken into account (TS_H-S *vs* TS_H-R), a preference for the transition state leading to the *wrong* enantiomer *S* would be predicted, since TS_H-S (Figure 1) is 1.8 kcal/mol lower in energy than its isomeric counterpart TS_H-R. The logical reason for it is that in TS_H-S, the nitrostyrene and the guanidine subunit are both found in the lower face of the enamine (from our view), adopting a less strained disposition. In contrast, the nitrostyrene and the guanidine lye in opposite faces of the enamine[19] in TS_H-R, and the structure needs to twist in order to form the internal H-bonds, adding some strain to the transition structure.

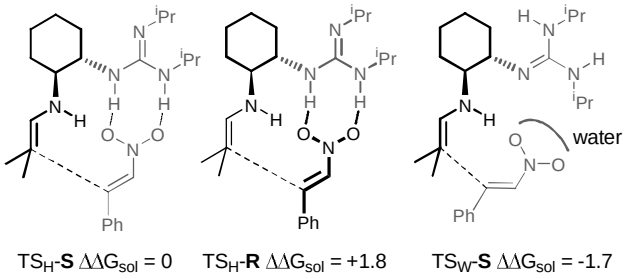

Figure 1. Comparison of guanidine activated transition states (TS_H-S and TS_H-R) with the water activated TS_W-S. Free Gibbs energies computed at B3LYP/6-311+G(d,p) (CPCM, water) level.

The clear disagreement of this finding with the experimental results can be understood as a first indication of the absence of intramolecular H-bonding in the reaction. Furthermore, confirming this hypothesis, we easily found a preliminary transition state (TS_W-S, Figure 1), in which the nitro group is activated by surrounding aqueous solvent (implicit water solvent model), with 1.7 kcal/mol lower activation energy than TS_H-S. Water might have a two-fold effect to lower the activation energy: it can solvate better the more polar transition state (TS_W-S *vs* TS_H-S), and it can form intermolecular hydrogen-bonds with the nitro group, accompanied by the disruption of the intramolecular ones.

If this is so, we should find a polar transition state, lacking intramolecular H-bonds, able to explain the preferential formation of the *R* enantiomer. It is worth to note at this point that the flexibility induced in the catalyst by the lack of internal hydrogen bonding restrictions, introduces some added difficulty to the calculations, due to a higher number of possible conformations in the transition states. Nonetheless, we were able to identify the two most stable conformations of the reactive enamine (Figures 2a and 2b), and finally the structures responsible for the formation of the *R* enantiomer.

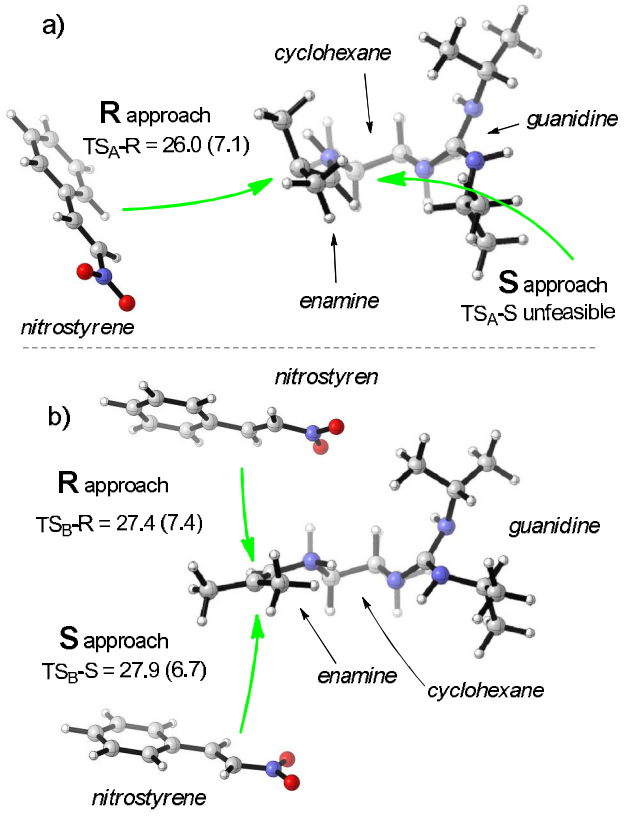

Figure 2. 3D-Models (based on computed transition states) for *R* and *S* approaches of styrene to the two most stable conformations of the enamine. Free Gibbs energies computed at B3LYP/6-311+G(d,p) (CPCM, water) [M06-2X/6-311+G(d,p) (SMD,water) in parenthesis].

Two theoretical approaching trajectories of the nitrostyrene to the catalyst (green arrows) are possible for each enamine. In Fig 2a, the face of the enamine[19] leading to the *S* enantiomer is blocked by the guanidine group, and the corresponding TS_A-S is not feasible, whilst in TS_A-R the nitrostyrene approaches from the unhindered side, leading to the transition state with the overall lowest activation energy ($\Delta G^{\ddagger}_{solv}$ = 26.0 kcal/mol, B3LYP functional). Meanwhile, the two faces of the other enamine (Figure 2b) present similar hindrance, affording transition states TS_B-R and TS_B-S of close energy (27.4 and 27.9 kcal/mol respectively). Thus, the preferential formation of the *R* enantiomer would arise from the predominance of the sum of TS_A-R and TS_B-R over TS_B-

S,[20] and the non-existence of TS_A-S. The steric effect of the guanidine group seems to be reason behind these observations.

3. Conclusions

We conclude that primary amine-guanidines, prepared by a simple monoguanylation of enantiomerically pure *trans*-cyclohexane-1,2-diamines act as organocatalysts in the enantioselective conjugate addition of isobutyraldehyde to nitroalkenes leading to enantiomerically enriched γ-nitroaldehydes. Good yields and enantioselectivities can be achieved working in aqueous solvents and in the presence of imidazole as rate-accelerating additive. Theoretical calculations suggest that the stereoinduction exerted by the guanidine arises from its capacity to block one of the faces of the reactive enamine in some of its reactive conformations, while water molecules activate the nitro group towards nucleophilic attack by hydrogen bonding and solvation of the polar transition state.

4. Experimental

4.1. General. All the reagents and solvents employed were of the best grade available and were used without further purification. The ^{1}H and ^{13}C NMR spectra were recorded at 25 ºC on a Bruker AC-300 at 300 MHz and 75 MHz, respectively, using TMS as internal standard. Nitroalkenes **8** were purchased or prepared according to a reported procedure.[21] Absolute configuration for adducts **9** were determined according to the described order of elution of their enantiomers in chiral HPLC. Reference racemic samples of adducts **9** were obtained by performing the reaction using 4-methylbenzylamine (20 mol%) as organocatalyst in toluene as solvent at 25 ºC.

4.2. General Procedure for the Enantioselective Michael Addition Reaction. To a solution of **6a,** *ent*-**6a** or **6b** (0.1 mmol), the nitroalkene (0.5 mmol) and imidazole (6.8 mg, 0.1 mmol) in DMF/H_2O (1/4, v/v) (1.25 mL) was added isobutyraldehyde (228 µL, 2.5 mmol) and the mixture was stirred at 0 ºC until reaction completion (TLC). The reaction was quenched with HCl 2N (10 mL) and the mixture was extracted with AcOEt (3x10 mL). The organic phase was washed with H_2O (2x10 mL), dried over $MgSO_4$, and the solvent was evaporated (15 Torr) to get the crude product, which was purified by silica gel chromatography (*n*-hexane/AcOEt gradients).

Adducts **9** were identified by comparison of their spectroscopic data with those of the literature. Their enantiomeric excesses were determined by chiral HPLC.

(*R*)-2,2-Dimethyl-4-nitro-3-phenylbutanal (9a).[17] ^{1}H NMR (300 MHz, $CDCl_3$): δ_H = 9.53 (s, 1H), 7.37-7.28 (m, 3H), 7.23-7.16 (m, 2H), 4.86 (dd, *J* = 13.0, 11.2 Hz, 1H), 4.69 (dd, *J* = 13.0, 4.3 Hz, 1H), 3.78 (dd, *J* = 11.2, 4.3 Hz, 1H), 1.14 (s, 3H), 1.01 (s, 3H) ppm; ^{13}C NMR (75 MHz, $CDCl_3$): δ_C = 204.3, 135.4, 129.2, 128.8, 128.3, 76.4, 48.6, 48.3, 21.8, 19.0 ppm; HPLC: Chiralcel OD-H, λ = 210 nm, *n*-hexane/2-propanol, 80:20, 0.7 mL/min, t_r (major) = 17.8 min, t_r (minor) = 24.5 min.

(*R*)-2,2-Dimethyl-4-nitro-3-(*p*-tolyl)butanal (9b).[17] ^{1}H NMR (300 MHz, $CDCl_3$): δ_H = 9.53 (s, 1H), 7.17-7.04 (m, 4H), 4.82 (dd, *J* = 12.9, 11.3 Hz, 1H), 4.67 (dd, *J* = 12.9, 4.2 Hz, 1H), 3.74 (dd, *J* = 11.3, 4.2 Hz, 1H), 2.32 (s, 3H), 1.13 (s, 3H), 1.01 (s, 3H) ppm; ^{13}C NMR (75 MHz, $CDCl_3$): δ_C = 204.5, 138.0, 132.2, 129.5, 129.0, 76.5, 48.3 (x2), 21.7, 21.1, 19.0 ppm; HPLC: Chiralcel OD-H, λ = 210 nm, *n*-hexane/2-propanol, 75:25, 0.8 mL/min, t_r (major) = 11.3 min, t_r (minor) = 15.5 min.

(*R*)-3-(4-Methoxyphenyl)-2,2-dimethyl-4-nitrobutanal (9c).[17] ^{1}H NMR (300 MHz, $CDCl_3$): δ_H = 9.53 (s, 1H), 7.15-7.08 (m, 2H), 6.89-6.82 (m, 2H), 4.81 (dd, *J* = 12.8, 11.3 Hz, 1H), 4.66 (dd, *J* = 12.8, 4.3 Hz, 1H), 3.79 (s, 3H), 3.73 (dd, *J* = 11.3, 4.3 Hz, 1H), 1.12 (s, 3H), 1.01 (s, 3H) ppm; ^{13}C NMR (75 MHz, $CDCl_3$): δ_C = 204.5, 159.4, 130.2, 127.2, 114.2, 76.6, 55.3, 48.5, 48.0, 21.7, 19.0 ppm; HPLC: Chiralcel OD-H, λ = 210 nm, *n*-hexane/2-propanol, 75:25, 0.8 mL/min, t_r (major) = 13.6 min, t_r (minor) = 20.0 min.

(*R*)-3-(4-Fluorophenyl)-2,2-dimethyl-4-nitrobutanal (9d).[17] ^{1}H NMR (300 MHz, $CDCl_3$): δ_H = 9.51 (s, 1H), 7.19 (m, 2H), 7.05-7.02 (m, 2H), 4.82 (dd, *J* = 13.1, 11.3 Hz, 1H), 4.68 (dd, *J* = 13.1, 4.2 Hz, 1H), 3.81-3.76 (dd, *J* = 11.3, 4.2 Hz, 1H), 1.13 (s, 3H), 1.01 (s, 3H) ppm; ^{13}C NMR (75 MHz, $CDCl_3$): δ_C = 204.1, 163.7, 161.2, 131.2 (x2), 130.7 (x2), 115.9, 115.6, 76.4, 48.2, 47.8, 21.7, 18.9 ppm; HPLC: Chiralcel OD-H, λ = 210 nm, *n*-hexane/2-propanol, 80:20, 0.8 mL/min, t_r (major) = 12.6 min, t_r (minor) = 21.5 min.

(*R*)-3-(4-Chlorophenyl)-2,2-dimethyl-4-nitrobutanal (9e).[17] ^{1}H NMR (300 MHz, $CDCl_3$): δ_H = 9.51 (s, 1H), 7.35-7.29 (m, 3H), 7.19-7.11 (m, 2H), 4.83 (dd, *J* = 13.1, 11.3 Hz, 1H), 4.69 (dd, *J* = 13.1, 4.2 Hz, 1H), 3.77 (dd, *J* = 11.3, 4.2 Hz, 1H), 1.13 (s, 3H), 1.02 (s, 3H) ppm; ^{13}C NMR (75 MHz, $CDCl_3$): δ_C = 203.9, 134.1, 130.5, 129.1, 76.3, 48.3, 48.0, 29.8, 21.9, 19.1 ppm; HPLC: Chiralcel OD-H, λ = 210 nm, *n*-hexane/2-propanol, 75:25, 0.8 mL/min, t_r (major) = 12.9 min, t_r (minor) = 20.0 min.

(*R*)-3-(4-Bromophenyl)-2,2-dimethyl-4-nitrobutanal (9f).[17] ^{1}H NMR (300 MHz, $CDCl_3$): δ_H = 9.49 (s, 1H), 7.48-7.45 (m, 2H), 7.11-7.08 (m, 2H), 4.81 (dd, *J* = 13.1, 11.3 Hz, 1H), 4.68 (dd, *J* = 13.1, 4.2 Hz, 1H), 3.78-3.73 (dd, *J* = 11.3, 4.2 Hz, 1H), 1.12 (s, 3H), 0.99 (s, 3H) ppm; ^{13}C NMR (75 MHz, $CDCl_3$): δ_C = 203.9, 134.5, 131.9, 130.8, 122.3, 76.1, 48.1, 47.9, 21.8, 18.9 ppm; HPLC: Chiralcel OD-H, λ = 210 nm, *n*-hexane/2-propanol, 80:20, 0.8 mL/min, t_r (major) = 16.4 min, t_r (minor) = 24.1 min.

(*R*)-2,2-Dimethyl-4-nitro-3-(4-nitrophenyl)butanal (9g).[17] ^{1}H NMR (300 MHz, $CDCl_3$): δ_H = 9.49 (s, 1H), 8.21 (m, 2H), 7.44 (m, 2H), 4.93 (dd, *J* = 13.1, 11.3 Hz, 1H), 4.81-4.76 (dd, *J* = 13.1, 4.2 Hz, 1H), 3.94 (dd, *J* = 11.3, 4.2 Hz, 1H), 1.16 (s, 3H), 1.05 (s, 3H) ppm; ^{13}C NMR (75 MHz, $CDCl_3$): δ_C = 203.2, 147.7, 143.4, 130.2, 123.9, 75.8, 48.2, 48.1, 21.8, 19.0 ppm; HPLC: Chiralcel OD-H, λ = 210 nm, *n*-hexane/2-propanol, 80:20, 0.7 mL/min, t_r (major) = 12.5 min, t_r (minor) = 20.9 min.

(*R*)-2,2-Dimethyl-3-(naphtalen-2-yl)-4-nitrobutanal (9h).[17] ^{1}H NMR (300 MHz, $CDCl_3$): δ_H = 9.55 (s, 1H), 7.80-7.75 (m, 3H), 7.70 (m, 1H), 7.50-7.45 (m, 2H), 7.28 (m, 1H), 4.97 (dd, *J* = 13.1, 11.3 Hz, 1H), 4.76 (dd, *J* = 13.1, 4.2 Hz, 1H), 3.97-3.92 (dd, *J* = 11.3, 4.2 Hz, 1H), 1.17 (s, 3H), 1.04 (s, 3H) ppm; ^{13}C NMR (75 MHz, $CDCl_3$): δ_C = 204.3, 133.3, 132.9 (x2), 128.5, 128.4, 127.9, 127.6, 126.6 (x2), 126.4, 76.4, 48.7, 48.5, 21.8, 19.0 ppm; HPLC: Chiralcel OD-H, λ = 210 nm, *n*-hexane/2-propanol, 80:20, 0.7 mL/min, t_r (minor) = 29.7 min, t_r (major) = 44.6 min.

(*R*)-2,2-Dimethyl-4-nitro-3-(pyridin-3-yl)butanal (9i).[22] ^{1}H NMR (300 MHz, $CDCl_3$): δ_H = 9.51 (s, 1H), 8.58-8.56 (m, 1H), 8.52-8.51 (m, 1H), 7.60-7.57 (m, 1H), 7.31-7.27 (m, 1H), 4.88 (dd, *J* = 13.7, 11.4 Hz, 1H), 4.75 (dd, *J* = 13.7, 4.1 Hz, 1H), 3.82 (dd, *J* = 11.4, 4.1 Hz, 1H), 1.15 (s, 3H), 1.05 (s, 3H) ppm; ^{13}C NMR (75 MHz, $CDCl_3$): δ_C = 203.4, 150.6, 149.6, 136.1, 131.4, 123.5, 75.7, 48.2, 46.0, 21.8, 18.9 ppm; HPLC: Chiralpak AD-H, λ = 210 nm, *n*-hexane/2-propanol, 80:20, 1 mL/min, t_r (minor) = 11.1 min, t_r (major) = 13.0 min.

(*R*)-3-(Furan-2-yl)-2,2-dimethyl-4-nitrobutanal (9j).[17] ^{1}H NMR (300 MHz, $CDCl_3$): δ_H = 9.52 (s, 1H), 7.38-7.37 (d, *J* = 1.6 Hz, 1H), 6.32-6.31 (dd, *J* = 5.2, 4.0 Hz, 1H), 6.22 (d, *J* = 3.2 Hz, 1H), 4.7 (dd, *J* = 12.8, 11.2 Hz, 1H), 4.58 (dd, *J* = 13.1, 4.2 Hz, 1H), 3.94-3.91 (dd, *J* = 11.3, 4.2 Hz, 1H), 1.18 (s, 3H), 1.05 (s, 3H) ppm; ^{13}C NMR (75 MHz, $CDCl_3$): δ_C = 203.5, 149.8, 142.8, 110.4, 109.7, 74.9, 48.2, 42.3, 21.1, 19.0 ppm; HPLC: Chiralcel OD-H, λ = 210 nm, *n*-hexane/2-propanol, 75:25, 0.8 mL/min, t_r (major) = 8.8 min, t_r (minor) = 13.2 min.

4.3. Calculations. All structures were initially optimized using the functional B3LYP and the 6-31G basis set as implemented in Gaussian 09,[23] and then reoptimized at B3LYP/6-311+G(d,p)[24] and M06-2X/6-311+G(d,p)[25] introducing solvent factors with the CPCM[26] model (solvent = water). The stationary points were characterized by frequency calculations in order to verify that they have the right number of imaginary frequencies. The intrinsic reaction coordinate (IRC)[27] were followed to verify the energy profiles connecting each transition structure to the correct associated local minima.

Acknowledgments

We thank the financial support from the Spanish Ministerio de Economía y Competitividad (projects CTQ2010-20387, CTQ2010-21263-C02 and Consolider Ingenio 2010, CSD2007-00006), FEDER, the COST Action CM0905 "Organocatalysis", the Generalitat Valenciana (Prometeo/2009/039), the Basque Government (GV grant IT-291-07), the FP7 Marie Curie Actions of the European Commission via the ITN ECHONET Network (MCITN-2012-316379) and the universities of Alicante and the Basque Country. We also thank SGI/IZO-SGIker UPV/EHU for allocation of computational resources.

References

1. (a) Ikeda, S.; Shibuya, M.; Kanoh, N.; Iwabuchi, Y. *Org. Lett.* **2009**, *11*, 1833-1836; (b) Zou, W.; Vembaiyan, K.; Bhasin, M.; Williams, D. T. *Carbohydr. Res.* **2009**, *344*, 2144-2150; (c) Pansare, S. V.; Lingampally, R.; Kirby, R. L. *Org. Lett*. **2010**, *12*, 556-559.
2. (a) Ma, H.; Liu, K.; Zhang, F.-G.; Zhu, C.-L.; Nie, J.; Ma, J.-A. *J. Org. Chem.* **2010**, *75*, 1402-1409; (b) Nakamura, A.; Lectard, S.; Hashizume, D.; Hamashima, Y.; Sodeoka, M. *J. Am. Chem. Soc.* **2010**, *132*, 4036-4037.
3. Szanto, G.; Hegedus, L.; Mattyasovszky, L.; Simon, A.; Simon, A.; Bitter, I.; Toth, G.; Toke, L.; Kadas, I. *Tetrahedron* **2009**, *65*, 8412-8417.
4. Andrey, O.; Vidonne, A.; Alexakis, A. *Tetrahedron Lett.* **2003**, *44*, 7901-7904.
5. Yu, Z.; Liu, X.; Zhou, L.; Lin, L.; Feng, X. *Angew. Chem., Int. Ed.* **2009**, *48*, 5195-5198.
6. Hong, B.-C.; Kotame, P.; Tsai, C.-W.; Liao, J.-H. *Org. Lett*. **2010**, *12*, 776-779.
7. (a) Elsner, P.; Jiang, H.; Nielsen, J. B.; Pasi, F.; Jørgensen, K. A. *Chem. Commun*. **2008**, 5827-5829; (b) Karthikeyan, T.; Sankararaman, S. *Tetrahedron: Asymmetry* **2008**, *19*, 2741-2745; (c) Ruiz, N.; Reyes, E.; Vicario, J. L.; Badia, D.; Carrillo, L.; Uria, U. *Chem. Eur. J.* **2008**, *14*, 9357-9367; (d) Krayer, M.; Ptaszek, M.; Kim, H.-J.; Meneely, K. R.; Fan, D.; Secor, K.; Lindsey, J. S. *J. Org. Chem.* **2010**, *75*, 1016-1039.
8. Reviews: (a) Berner, O. M.; Tedeschi, L.; Enders, D. *Eur. J. Org. Chem.* **2002**, 1877-1894. (b) Almaşi, D.; Alonso, D. A.; Nájera, C. *Tetrahedron: Asymmetry* **2007**, *18*, 299-365; (c) Tsogoeva, S. B. *Eur. J. Org. Chem*. **2007**, 1701-1716. (d) Aitken, L. S.; Arezki, N. R.; Dell'Isola, A.; Cobb, A. J. A. *Synthesis* **2013**, 2627-2648.
9. Recent review: Serdyuk, O. V.; Heckel, C. M.; Tsogoeva, S. B. *Org. Biomol. Chem*. **2013**, *11*, 7051-7071.
10. Zhang, X.-J.; Liu, S.-P.; Lao, J.-H.; Du, G.-J.; Yan M.; Chan, A. S. C. *Tetrahedron: Asymmetry* **2009**, *20*, 1451-1458.
11. Uehara H.; Barbas III, C. F. *Angew. Chem., Int. Ed.* **2009**, *48*, 9848-9852.
12. Lalonde, M. P.; Chen Y.; Jacobsen, E. N. *Angew. Chem., Int. Ed.* **2006**, *45*, 6366-6370.
13. Chen, J.-R.; Zou, Y.-Q.; Fu, L.; Ren, F.; Tan, F.; Xiao, W.-J. *Tetrahedron* **2010**, *66*, 5367-5372.

14. Ma, Z.-W.; Liu, Y.-X.; Zhang, W.-Z.; Tao, Y.; Zhu, Y.; Tao, J.-C.; Tang, M. S. *Eur. J. Org. Chem.* **2011**, 6747-6754.
15. Durmaz, M.; Sirit, A. *Supramol. Chem*. **2013**, *25*, 292-301.
16. (a) Avila, A.; Chinchilla, R.; Nájera, C. *Tetrahedron: Asymmetry* **2012**, *23*, 1625–1627; (b) Avila, A.; Chinchilla, R.; Gómez-Bengoa, E.; Nájera, C. *Eur. J. Org. Chem.* **2013**, 5085-5092.
17. Bai, J.-F.; Xu, X.-Y.; Huang, Q.-C.; Peng, L.; Wang, L.-X. *Tetrahedron Letters* **2010**, *51*, 2803-2805.
18. (a) Seebach, D.; Golinski, J. *Helv. Chim. Acta* **1981**, *64*, 1413-1423; (b) Seebach, D.; Beck, A. K.; Golinski, J.; Hay, J. N.; Laube, T. *Helv. Chim. Acta* **1985**, *68*, 162-172.
19. Seebach´s model is diastereospecific (see ref. 18), meaning that each reacting face of the enamine determines the approaching face of the nitrostyrene, and thus the sense of the enantioinduction.
20. It is worth noting the notorious difference in activation energies between B3LYP (26-28 kcal/mol) and M06-2X (6-7 kcal/mol) functionals, and the fact that the energies of the three transition states are within computational error with M06-2X (7.1, 7.4, 6.7 kcal/mol), restricting the explanation with this functional to the qualitative difference of approaching trajectories drawn in Figure 2.
21. Rodríguez, J. M.; Pujol, M. D. *Tetrahedron Lett.* **2011**, *52*, 2629-2632.
22. Yoshida, M.; Sato, A.; Hara, S. *Org. Biomol. Chem.* **2010**, *8*, 3031-3036.
23. Frisch, M. J.; Trucks, G. W.; Schlegel, H. B.; Scuseria, G. E.; Robb, M. A.; Cheeseman, J. R.; Scalmani, G.; Barone, V.; Menucci, B., Petersson, G. A.; Nakatsuji, H.; Caricato, M.; Li, X.; Hratchian, H. P.; Izmaylov, A. F.; Bloino, J.; Zheng, G.; Sonnenberg, J. L.; Hada, M.; Ehara, M.; Toyota, K.; Fukuda, R.; Hasegawa, J.; Ishida, M.; Nakajima, T.; Honda, Y.; Kitao, O.; Nakai, H.; Vreven, T.; Montgomery, J. A., Jr.; Peralta, J. E.; Ogliaro, F.; Bearpark, M.; Heyd, J. J.; Brothers, E.; Kudin, K. N.; Staroverov, V. N.; Kobayashi, R.; Normand, J.; Raghavachari, K.; Rendell, A.; Burant, J. C.; Iyengar, S. S.; Tomasi, J.; Cossi, M.; Rega, N.; Millam, J. M.; Klene, M.; Knox, J. E.; Cross, J. B.; Bakken, V.; Adamo, C.; Jaramillo, J.; Gomperts, R.; Stratmann, R. E.; Yazyev, O.; Austin, A. J.; Cammi, R.; Pomelli, C.; Ochterski, J. W.; Martin, R. L.; Morokuma, K.; Zakrewski, V. G.; Voth, G. A.; Salvador, P.; Dannenberg, J. J.; Dapprich, S.; Daniels, A. D.; Farkas, O.; Foresman, J. B.; Ortiz, J. V.; Cioslowski, J.; Fox, D. J. Gaussian 09, Revision A.02, Gaussian Inc., Wallingford CT, 2009.
24. Lee, C.; Yang, W.; Parr, R. G. Phys. Rev. B 1988, 37, 785–789; (b) Becke, A. D. *J. Chem. Phys.* **1993**, *98*, 5648–5652; (c) Kohn, W.; Becke, A. D.; Parr, R. G. *J. Phys. Chem.* **1996**, *100*, 12974–12980.
25. Zhao, Y.; Truhlar, D. G.; *Theor. Chem. Acc.*, **2008**, *120*, 215-241.
26. (a) Cancès, E.; Mennucci, B.; Tomasi, J. *J. Chem. Phys.* **1997**, *107*, 3032–3047; (b) Tomasi, J.; Mennucci, B.; Cancès, E. *J. Mol. Struct. (Theochem)* **1999**, *464*, 211–226.
27. González, C.; Schlegel, H. B. *J. Phys. Chem.* **1990**, *94*, 5523–5527.